JOURNAL OF MATERIALS SCIENCE 31 (1996) 649–654

Microstructure and oxidation resistance of SiC coated carbon–carbon composites via pressureless reaction sintering

CHEN-CHI M. MA*[‡], NYAN-HWA TAI*, WEN-CHI CHANG, HUAI-TE CHAO
*Institute of Chemical Engineering and *Materials Science Center, National Tsing-Hua University, Hsinchu, Taiwan, 30 043, People's Republic of China*

The effects of processing parameters on the microstructure and oxidation resistance of silicon carbide (SiC) coated carbon–carbon (C–C) composites were investigated. C–C composites were made from plain woven carbon cloths and phenolic derived carbon matrices in the laboratory. Pressureless reaction sintering has been used to apply SiC coating to C–C composites using epoxy resin and silicon powder as the precursor. Results showed that the oxidation resistance of C–C composites was enhanced by coating with SiC. The pressureless reaction sintering process exhibits good processability. β-SiC was formed after heat treatment at 1800 °C and the α-SiC formed after heat treatment at 2200 °C. The SiC coated C–C composites exhibit good oxidation resistance at 1000 °C for 100 h under the test conditions.

1. Introduction

Carbon fibre reinforced carbon matrix material (carbon–carbon composite, C–C) has been a leading candidate material for high temperature applications due to its outstanding characteristics, including high strength at elevated temperature, low density, high vaporization temperature, multiformity and thermal shock resistance [1–9]. However, a serious drawback, which restricts the application of C–C composites in non-oxidation environments, is the poor oxidation resistance of carbon that will react with oxygen and burn away rapidly above 500 °C [2, 4, 9–11]. The fundamental requirements for protecting C–C composites from oxidation include:

1. providing an effective barrier to inward diffusion of oxygen and outward diffusion of carbon,
2. possessing low volatility to prevent excessive erosion in high velocity gas stream,
3. achieving good adherence to the substrate, and
4. exhibiting chemical and mechanical compatibility [9–13].

Several approaches [11–39] have been considered to prevent carbon materials from oxidation. Two conventional methods to improve the oxidation resistance of the C–C composites are (a) adding inhibitors into the carbon matrix to slow down the carbon oxidation rate [14–20], and (b) coating protective ceramic materials on the surface of C–C composites to encapsulate the composites and to prevent oxygen from reacting with underlying carbon materials [11, 13, 21–39]. Although there have been lots of efforts for oxidation protection on C–C composites, their achievements are far from requirement. Silicon carbide has been widely selected as a protective coating layer for anti-oxidation applications [26–38] for its good chemical compatibility with underlying carbon substrate, low thermal expansion coefficient and can survive under an oxidation environment at about 1650 °C.

The silicon carbide layer could be formed via the chemical vapour deposition method [26–35], silicon carbide powder coating [40] and reaction sintering methods [37, 39, 41, 42], etc. SiC coating layer by the reaction sintering method is one of the more suitable processes to achieve good interfacial adhesion with C–C composite substrates. The sintering aids, sintering time and temperature may affect the sintering efficiency and the thickness of coating layer [42–45]. The objective of this paper is to study the processability of SiC coated C–C composite via pressureless reaction sintering. The microstructure of the coating layer and oxidation resistance of the coated C–C composite are also investigated, respectively.

2. Experimental procedure

2.1. Material preparation

The unidirectional C–C composites used in this study were made from PAN based carbon fibres and a carbonized phenolic matrix by a wet drum winding method. After carbonization, the density of the C–C composite was about 1.5 g cm^{-3}. C–C composites were cut into 20 × 10 × 3 mm blocks. Before

---

[‡] To whom all correspondence should be addressed.

0022–2461 © *1996 Chapman & Hall*

the coating process, the samples were cleaned in acetone by ultrasonication.

2.2. Coating processes

The coating solution, including 40–60 wt % silicon powder (325 mesh), 2–3 wt % boron powder (400 mesh), 30–50 wt % epoxy resin (DER331), 3–5 wt % diethyltoluenediamine (DETDA) and solvents, were applied on the C–C substrates by an air spraying method. In the coating process, silicon powder was used as the raw material, boron was used as a sintering aid, epoxy resin was a binder and carbon source, and DETDA was utilized as a curing agent.

The coated specimens were placed in a hood for 12 h; then, the curing of epoxy resin was performed in an oven at 130 °C for 2 h and at 150 °C for 2 h, with a heating rate of 10 °C h^{-1}.

2.3. Sintering process

Pressureless reaction sintering processes were carried out at 1800, 2200 and 2600 °C in an inert gas environment at atmospheric pressure. During the sintering process the specimens were placed in a graphite crucible with a graphite lid on it.

2.4. Coating characterization

Formation of the silicon carbide layer converted from a silicon powder–epoxy resin mixture was investigated by X-ray diffraction (XRD Shimadzn XD-3A, with CuK_α radiation at 30 kV and 20 mA). The morphologies of the surface and cross-sectional specimens were observed by scanning electron microscopy (Joel, 840A). The electron probe X-ray microanalyser (Joel, JXA-8800M) was used to inspect the distribution of the silicon atom.

2.5. Oxidation resistance evaluation

In this study, isothermal and dynamic oxidation methods were adopted for the evaluation of oxidation behaviour of the coated and uncoated C–C composites. A diagram of the thermogravimetric measurement apparatus is shown in Fig. 1. The isothermal oxidation tests were performed at 1000 °C in flowing air. Relationships between weight loss and oxidation time were obtained from the isothermal oxidation tests. The dynamic oxidation tests were carried out at a heating rate of 5 °C $\min^{-1}$ from room temperature to 1100 °C. Weight–time data collected from the computer were converted to an oxidation rate–oxidation temperature relationship after suitable processes.

3. Results and discussion

3.1. X-ray pattern of surface coatings

The peak of the (0 0 2) plane of the C–C composites substrate is shown in Fig. 2. After coating, sharp peaks which appeared around 28, 47 and 56 ° reflect peaks diffracted from the silicon structure (1 1 1), (2 2 0) and (3 1 1) planes, respectively (as shown in Fig. 3). Since the silicon–epoxy coatings encapsulate the C–C composite, the diffraction peaks of the carbon structure cannot be detected clearly after the coating process by XRD.

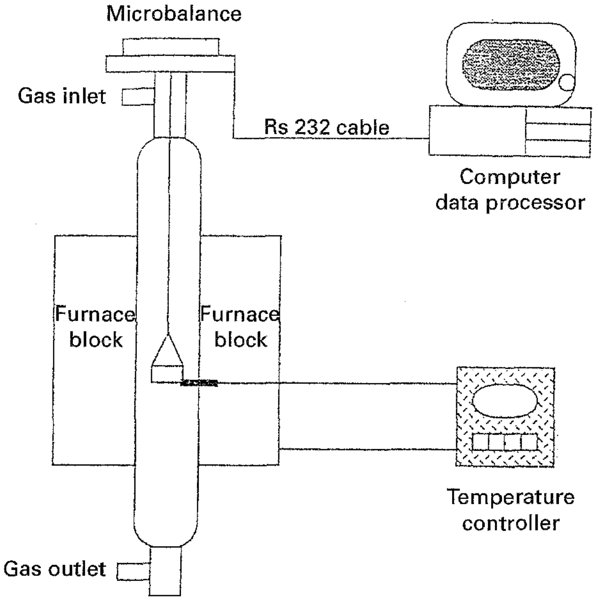

Figure 1 Schematic diagram of the instrument for measuring the sample weight loss at high temperature.

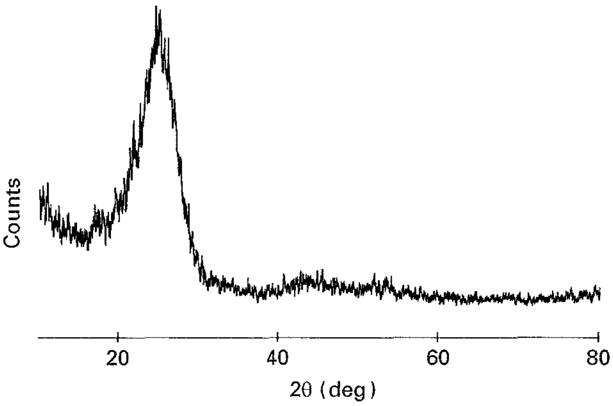

Figure 2 XRD pattern of uncoated C–C composite.

After sintering at 1800 °C, the peaks around 28, 47 and 56 ° disappeared. New peaks shifted to 35, 41 and 60 °, respectively (as shown in Fig. 4). These peaks are the typical diffraction peaks of the (1 1 0), (2 0 0) and (2 2 0) planes of the silicon carbide structure. Based upon the result of the XRD pattern, no silicon powder diffraction pattern is observed. Thus, it might be concluded that the silicon powders reacted with the carbon atom resulting in the formation of silicon carbide. Furthermore, the sharper and narrower diffraction peak of the (0 0 2) plane of the carbon structure implies that the structure of the C–C composite became more perfect after heat treatment at 1800 °C.

Once the sintering temperature increased, the silicon carbide transformed to a different crystalline structure. Fig. 5 is the XRD pattern of coated C–C composites sintered at 2200 °C. There is a discrepancy between the diffraction peaks of the C–C composites

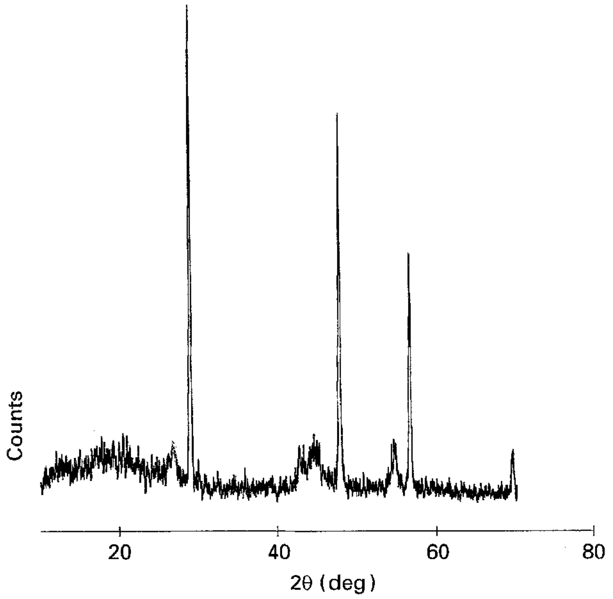

Figure 3 XRD pattern of C–C composite coated with epoxy–silicon coating.

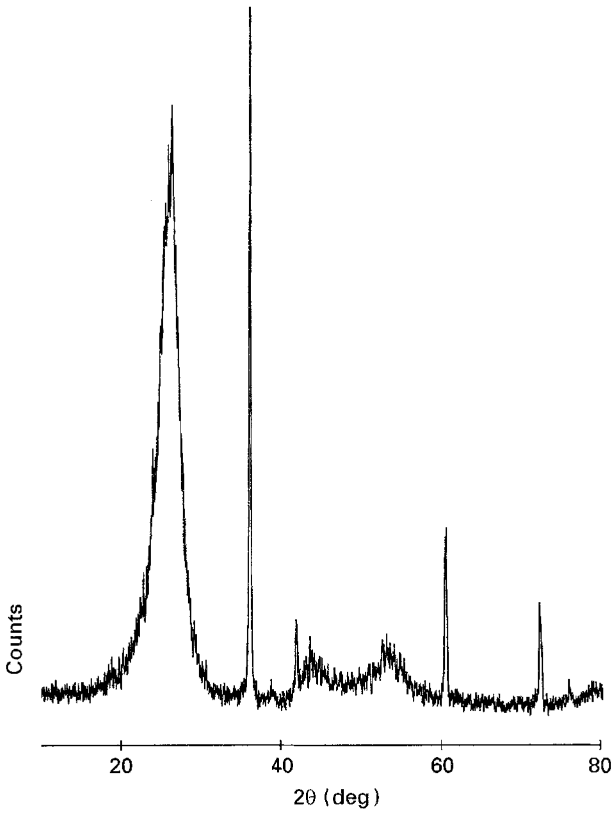

Figure 4 XRD pattern of C–C composite coated with SiC following 1800 °C sintering.

sintered at 1800 and 2200 °C. The significant difference is the peak around 35 °. Only a single strong peak around 35 ° is observed for the coated C–C composite sintered at 1800 °C. However, the diffraction peak splits into three peaks for the coated C–C composite sintered at 2200 °C. The difference is due to the change of the crystalline silicon carbide structure after heat treatment at 2200 °C. There are two main crystal forms for silicon carbide [46] : one is the cubic form (β-SiC); the other is the hexagonal form (α-SiC). The hexagonal form of silicon carbide would result in the splitting of diffraction peaks around 35 °. Based upon the XRD pattern, it shows that the β-SiC structure could be formed on the C–C composite surface at 1800 °C by the pressureless reaction sintering method; on the other hand, the α-SiC structure can be formed at 2200 °C by the same process.

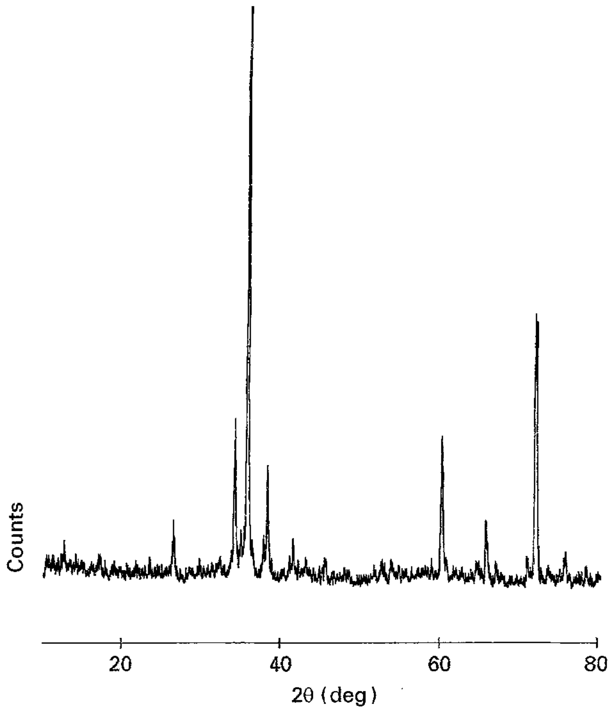

Figure 5 XRD pattern of C–C composite coated with SiC following 2200 °C sintering.

3.2. Morphology and atom distribution of silicon and carbon atoms on coated C–C composites

The cross-sectional morphologies of the uncoated C–C composite and of the C–C composite coated with silicon carbide are shown in Figs 6 and 7, respectively. The thickness of the silicon carbide coating is about 8 μm, as measured from Fig. 7. The surface morphology of the C–C composite coated with silicon–epoxy is shown in Fig. 8. A rougher coated C–C composite surface was observed when the silicon–epoxy coating was treated at 1800 °C. The C–C composite with a silicon–epoxy coating shows a smoother surface, and the coating encapsulates the C–C substrate uniformly. Silicon powders (white region) are distributed in the epoxy resin (dark region) over the C–C composites, as can be seen in Fig. 8.

After heat treatment at 1800 °C, the silicon–epoxy coating converts to a relatively rough silicon carbide

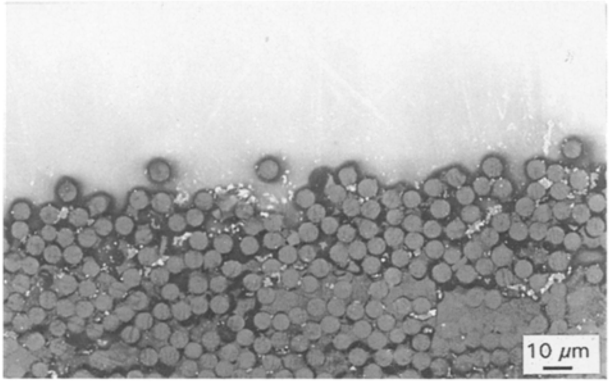

Figure 6 The cross-sectional morphology of uncoated C–C composite.

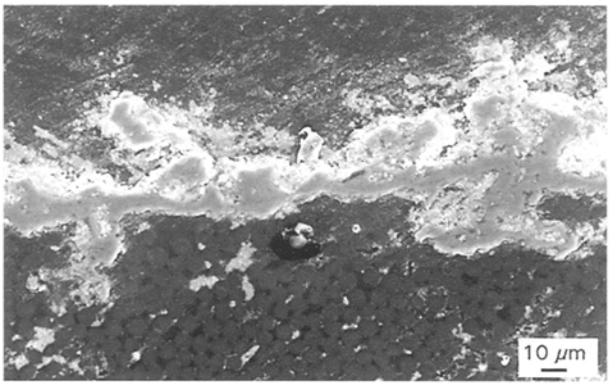

Figure 7 The cross-sectional morphology of C–C composite coated with SiC.

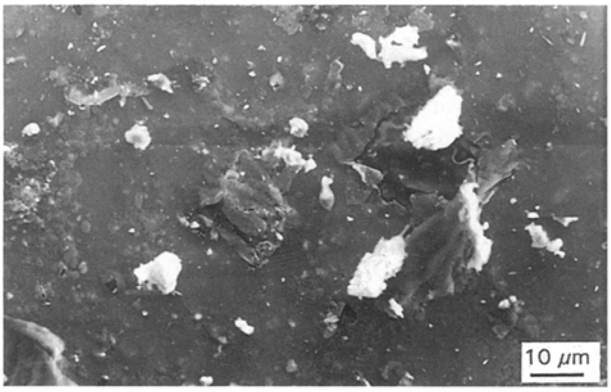

Figure 8 The surface morphology of C–C composite with silicon–epoxy coating.

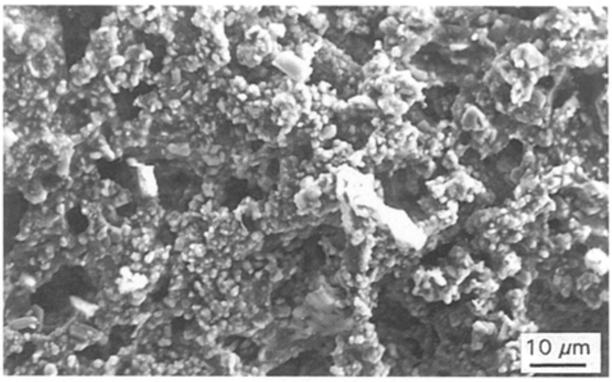

Figure 9 The surface morphology of C–C composite coated with SiC after 1800 °C sintering.

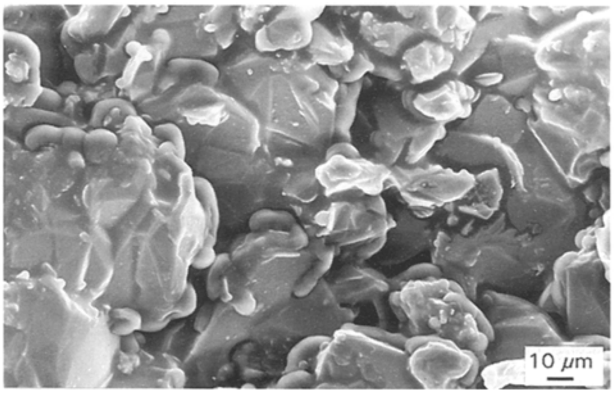

Figure 10 The surface morphology of C–C composite coated with SiC after 2200 °C sintering.

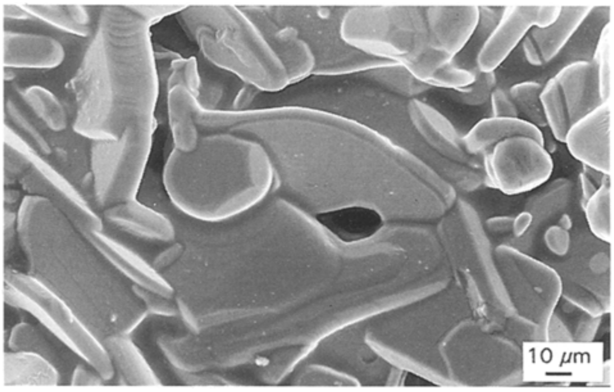

Figure 11 The surface morphology of C–C composite coated with SiC after 2600 °C sintering.

layer (as shown in Fig. 9). The rough surface may be caused by any of the following: evolution of a gas by-product during pyrolysis of epoxy resin; the original rough surface of the C–C composites; and the silicon carbide granulation process. Based upon the XRD pattern, no carbon peak is detected, implying that the silicon carbide structure has been built up on the C–C composite surface. A dense silicon carbide structure can be obtained after a proper sintering process. A dense coated layer possesses high strength at elevated temperature, high resistance to thermal shock and good thermal conductivity. The higher heat treatment temperatures at 2200 and 2600 °C were applied in this study to obtain an SiC coated layer with better properties. The surface morphologies of the silicon carbide coatings after sintering at 2200 and 2600 °C are illustrated in Figs 10 and 11, respectively. Obvious grain growth is detected on the SiC layer as the temperature increased from 2200 to 2600 °C. A denser surface morphology was obtained at higher sintering temperatures. The grain size of SiC increases with increasing sintering temperature, reducing the voids between small grain boundaries.

From the examination of the distribution of silicon atoms on the C–C composite substrate, the formation of silicon carbide from silicon powder can be seen. Fig. 12 shows the silicon atom distribution on the C–C composite coated with silicon powder and epoxy

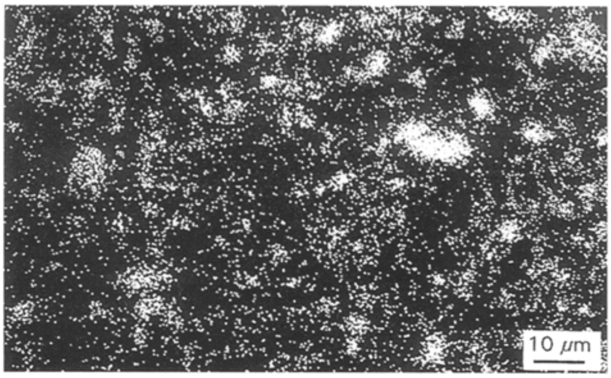

Figure 12 Silicon atom distribution on C–C composites with silicon–epoxy coating.

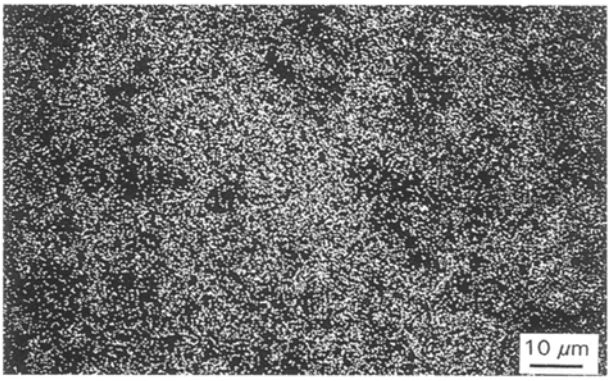

Figure 13 Silicon atom distribution on C–C composites coated with SiC following 1800 °C sintering.

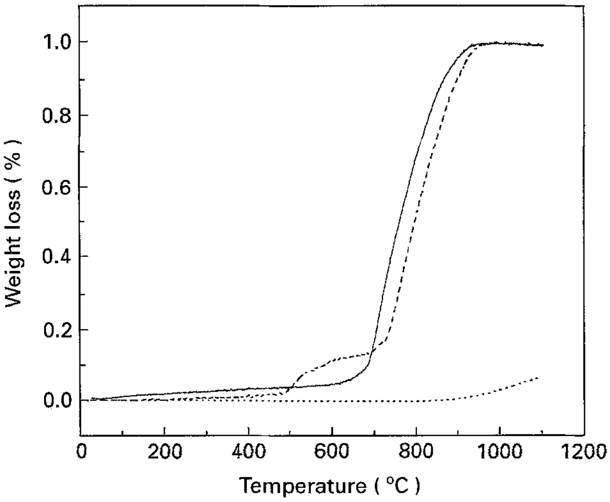

Figure 14 The weight loss of C–C composites in the non-isothermal oxidation test with a heating rate of 5 °C $\min^{-1}$. (—) uncoated C–C composite, (– – –) C–C composite coated with epoxy and Si, (···) C–C composite coated converted SiC.

resin (corresponding to the SEM photograph illustrated in Fig. 8). The strong aggregation of silicon atoms in the silicon–epoxy coatings are indicated as white dots in Fig. 12. Fig. 13 explains the distribution of silicon atoms on C–C composites coated with a silicon carbide layer. The distribution of silicon atoms is more uniform after sintering. The sintering temperature (above 1800 °C) is higher than the melting point of silicon (around 1410 °C). The molten silicon may flow freely and react with carbon to form a uniform silicon carbide layer during the sintering process. The SiC layer formed wraps the C–C composite, forming an oxygen insulation layer.

3.3. Evaluation of oxidation resistance

In this research, an investigation of oxidation resistance on various C–C composites was performed through isothermal and non-isothermal methods. The profiles of weight loss of uncoated C–C composite, of C–C composite coated with silicon–epoxy, and of C–C composite coated with converted silicon carbide are shown in Fig. 14. Drastic oxidation reaction of the uncoated C–C composite at temperatures over 550 °C is observed; however, no significant weight loss below 550 °C was detected. The slight weight loss is derived from the oxidation reaction of the defect carbon structure on the surface of the C–C composite. The oxidation rate increased with temperature up to 700 °C. Two controlling mechanisms for carbon oxidation reactions were proposed: surface reaction and gaseous diffusion. The surface reaction controlling step occurs at the temperature range 550–700 °C for uncoated C–C composites. A constant rate of weight loss is maintained above 700 °C. This implies that oxidation reactions above 700 °C are controlled by gaseous diffusion. The oxidation rate of the specimen could be measured by differentiating the weight loss. The activation energy of the oxidation reaction for uncoated C–C composites measured was 50 kcal mol^{-1}, which is comparable to the data published [47].

No significant weight loss is observed for the C–C composite coated with silicon–epoxy until 400 °C. The weight loss between 400 and 550 °C is due to epoxy burn out. The tendencies of weight loss profiles for C–C composites without coating and with silicon–epoxy coating above 700 °C are almost the same.

There is almost no weight loss for the C–C composite coated with converted silicon carbide up to 900 °C. This implies that the silicon carbide coatings can protect the C–C composites up to 900 °C. The constant weight loss above 1000 °C might be attributed to the oxidation reaction of non-perfect silicon carbide surface structures.

An oxidation resistance test at 1000 °C was performed in this study. The weight loss profiles of the uncoated C–C composite and the C–C composite coated with converted silicon carbide are shown in Fig. 15. The uncoated C–C composite was totally oxidized and converted to gaseous species (CO, CO_2) within 1 h. A uniform weight loss was detected for the SiC coated C–C composite during the first 8 h; however, no significant weight change of the specimen was observed in subsequent oxidation tests. The weight loss during the first 8 h test might be attributed to the oxidation of uncompleted surface structure. After 8 h oxidation, no weight change of the protected C–C composites was observed in further oxidation tests up to 100 h. Based upon these results, it may conclude that the oxidation resistance of the C–C composite with a converted silicon carbide protected layer is enhanced up to 1000 °C.

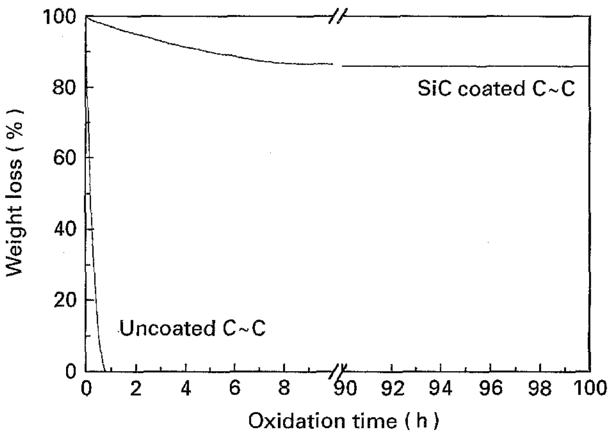

Figure 15 The weight loss of C–C composites in 1000 °C isothermal oxidation test.

4. Conclusions

SiC coated C–C composites made by pressureless reaction sintering processes are developed. The SiC coating is converted via pressureless reaction sintering using epoxy resin and silicon powder as precursor. A β-SiC structure was found by XRD after heat treatment at 1800 °C; meanwhile, an α-SiC structure was observed after heat treatment at 2200 °C. A smoother surface can be achieved after sintering at 2200 °C. The uncoated C–C composites begin to oxidize at 550 °C and burn out within 60 min in the atmosphere. However, the weight of the SiC coated C–C composite does not change until 900 °C, and only slight weight loss is observed at 1000 °C. In the isothermal oxidation test at 1000 °C, the SiC coated C–C composite shows 10% weight loss within the first 10 h and does not change any more within 100 h of the test.

5. Acknowledgement

This research was financially supported by National Science Council, Taiwan, R.O.C., under contract No. NSC 82-0405-E-007-261.

References

1. E. FITZER and W. HUTTNER, *J. Phys. D: Appl. Phys.* **14** (1981) 347.
2. E. FITZER, *Carbon* **25** (1987) 163.
3. *Idem, Pure & Appl. Chem.* **60** (1988) 287.
4. J. D. BUCKLEY, *Ceram. Bull.* **67** (1988) 364.
5. A. J. KLEIN, *Adv. Compos.* **4** (1989) 38.
6. C. F. LEWIS, *Mater. Eng.* **106** (1989) 27.
7. R. WEISS, in International Symposium on Carbon 1990, Tsukuba, November 1990, edited by M. Inagaki (Carbon Society of Japan, Tokyo, 1990), Plenary C, pp. 10–15.
8. G. W. MEETHAM, *J. Mater. Sci.* **26** (1991) 853.
9. G. SAVAGE, "Carbon–Carbon Composites" (Chapman & Hall, London, 1993) pp. 137–9.
10. P. R. BECKER, *Ceram. Bull.* **60** (1981) 1210.
11. J. R. STRIFE and J. E. SHEEHAN, *ibid.* **67** (1988) 369.
12. K. L. LUTHRA, *Carbon* **26** (1988) 217.
13. D. W. McKEE, *ibid.* **25** (1987) 551.
14. *Idem, ibid.* **24** (1986) 737.
15. C. T. HO and D. D. L. CHUNG, *ibid.* **28** (1990) 815.
16. S. RAGAN and G. T. EMMERSON, in Extended Abstracts and Program, 20th Biennial Conference on Carbon, Santa Barbara, CA, July 1991 (Electrochemical Society Inc., Manchester, NH, 1991) p. 339.
17. S. RAGAN and G. T. EMMERSON, *ibid.* p. 428.
18. J. W. DAVIS and A. A. HAAS, *J. Nucl. Mater.* **195** (1992) 166.
19. W. KOWBEL, Y. HUANG and H. TSOU, *Carbon* **31** (1993) 355.
20. A. J. LUCCHESI, J. C. HAY and K. W. WHITE, *J. Mater. Res.* **7** (1992) 1795.
21. J. COVINO, K. KLEMM and J. DYKEMA, *Mater. Perf.* **30** (1991) 75.
22. M. D. ALVEY and P. M. GEORGE, *Carbon* **29** (1991) 523.
23. K. MUMTAZ, J. ECHIGOYA, T. HIRAI and Y. SHINDO, *J. Mater. Sci. Lett.* **12** (1993) 1411.
24. K. MUMTAZ, J. ECHIGOYA and M. TAYA, *J. Mater. Sci.* **28** (1993) 5521.
25. J. P. QIAN, X. LIU, P. Y. LI and Z. GUO, *J. Nucl. Mater.* **191** (1992) 340.
26. K. SUGIYAMA and E. YAMAMOTO, *J. Mater. Sci.* **24** (1989) 3756.
27. D. KEHR, K. BRENNFLECK and R. WEISS, *High Temp. - High Press.* **22** (1990) 693.
28. F. J. BUCHANAN and J. A. LITTLE, *Surf. Coat. Technol.* **46** (1991) 217.
29. *Idem., ibid.* **53** (1992) 137.
30. T. M. WU, W. C. WEI and S. E. HSU, *Mater. Chem. Phys.* **33** (1993) 208.
31. W. LIU, S. SUN, M. LI and Y. WEI, *J. Mater. Sci. Lett.* **12** (1993) 886.
32. Y. K. KING and J. Y. LEE, *Carbon* **31** (1993) 1031.
33. F. J. BUCHANAN and J. A. LITTLE, *J. Mater. Sci.* **28** (1993) 2324.
34. H. MAHFUZ, P. S. DAS, S. JEELANI, D. M. BAKER and S. A. JOHNSON, *ibid.* **28** (1993) 5880.
35. F. J. BUCHANAN and J. A. LITTLE, *Corr. Sci.* **35** (1993) 1243.
36. H. MAHFUZ, D. XUE, S. JEELANI, D. M. BAKER and S. A. JOHNSON, *Comp. Sci. Technol.* **50** (1994) 411.
37. T. M. WU, W. C. WEI and S. E. HSU, *Carbon* **29** (1991) 1257.
38. *Idem, J. Euro. Ceram. Soc.* **9** (1992) 351.
39. *Idem, Ceram. Int.* **18** (1992) 167.
40. J. W. PATTEN, R. W. MOSS and B. A. FORCHT, US Patent 4 500 602 (1985).
41. T. M. WU, W. C. WEI and S. E. HSU, *Chinese J. Mater. Sci.* **22** (1990) 70.
42. M. KONDO, T. MORIMOTO, A. KOHYAMA and H. TSUNAKAWA, in ICCM-9, Vol. III, edited by A. Miravete (Woodhead Publishing, Machid, 1993) 703.
43. A. N. SHURSHAKOV, in "Refractory Carbides", edited by G. V. Samsnov (Consultants Bureau, NY, 1974) pp. 125–32.
44. K. NEGITA, *J. Amer. Ceram. Soc.* **69** (1986) 308.
45. G. H. WROBLEWSKA, *Ceram. Int.* **16** (1990) 201.
46. R. W. OLESINSKI, *Bull. Alloy Phase Diag.* **5** (1984) 486.
47. P. L. WALKER, *Carbon* **29** (1991) 411.

Received 4 October 1994
and accepted 8 June 1995